Published in final edited form as:
Sci Transl Med. 2010 August 18; 2(45): 45ra60. doi:10.1126/scitranslmed.3001002.

Multivalent Integrin-Specific Ligands Enhance Tissue Healing and Biomaterial Integration

Timothy A. Petrie[1,2], **Jenny E. Raynor**[3], **David W. Dumbauld**[1,2], **Ted T. Lee**[1,2], **Subodh Jagtap**[3], **Kellie L. Templeman**[1,2], **David M. Collard**[3], and **Andrés J. García**[1,2,*]

[1] Woodruff School of Mechanical Engineering, Georgia Institute of Technology, 315 Ferst Drive, Room 2314 IBB, Atlanta, GA 30332-0363, USA

[2] Petit Institute for Bioengineering and Bioscience, Georgia Institute of Technology, Atlanta, GA 30332, USA

[3] School of Chemistry and Biochemistry, Georgia Institute of Technology, Atlanta, GA 30332, USA

Abstract

Engineered biointerfaces covered with biomimetic motifs, including short bioadhesive ligands, are a promising material-based strategy for tissue repair in regenerative medicine. Potentially useful coating molecules are ligands for the integrins, major extracellular matrix receptors that require both ligand binding and nanoscale clustering for maximal signaling efficiency. We prepared coatings consisting of well-defined multimer constructs with a precise number of recombinant fragments of fibronectin (monomer, dimer, tetramer, and pentamer) to assess how nanoscale ligand clustering affects integrin binding, stem cell responses, tissue healing, and biomaterial integration. Clinical-grade titanium was grafted with polymer brushes that presented monomers, dimers, trimers, or pentamers of the $\alpha_5\beta_1$ integrin–specific fibronectin III (7 to 10) domain ($FNIII_{7–10}$). Coatings consisting of trimers and pentamers enhanced integrin-mediated adhesion in vitro, osteogenic signaling, and differentiation in human mesenchymal stem cells more than did surfaces presenting monomers and dimers. Furthermore, ligand clustering promoted bone formation and functional integration of the implant into bone in rat tibiae. This study establishes that a material-based strategy in which implants are coated with clustered bioadhesive ligands can promote robust implant-tissue integration.

INTRODUCTION

An overarching goal in materials engineering and medicine is the development of biomaterials to control cell function in order to promote tissue healing and regeneration (1, 2). Cell-biomaterial interactions are primarily governed by cell adhesion, which arises from the binding of cellular integrin receptors to biomacromolecules adsorbed, tethered, or deposited onto a surface or the extracellular matrix (3). Engagement of distinct integrin αβ heterodimers activates specific signaling pathways that regulate survival, proliferation, and phenotypic cellular programs (4, 5). For instance, binding of cell surface integrin to

*To whom correspondence should be addressed. andres.garcia@me.gatech.edu.

Author contributions: T.A.P., J.E.R., D.W.D., T.T.L., S.J., and K.L.T. contributed to collection of experimental data; T.A.P. and A.J.G. analyzed the data; T.A.P., D.M.C., and A.J.G. contributed to writing the paper.

Competing interests: A.J.G. has consulted for Synthes Inc. Georgia Tech Research Corporation has applied for a U.S. patent on the use of $FNIII_{7–10}$ for orthopedic repair. The authors declare that they have no competing interests.

extracellular fibronectin promotes osteoblast survival, cell cycle progression, differentiation, and matrix mineralization (6–9). Strategies to control integrin-mediated adhesion to bioinspired materials have been developed to regulate tissue repair and maintenance. For example, presentation of short oligopeptides such as the Arg-Gly-Asp (RGD) sequence derived from fibronectin on substrates allows for the selective activation of integrin signaling pathways (for example, $\alpha_v\beta_3$-mediated signaling by RGD) (2, 10–12). Other approaches make use of macromolecular ligands, including extracellular matrix–derived proteins such as collagen, elastin, and fibronectin (11, 12). These strategies have typically relied on the immobilization of the bioadhesive ligand onto a solid support in a relatively static arrangement, without the possibility of substantial ligand mobility or directed receptor clustering. This presentation is in contrast to the state of cell membrane integrin receptors, which are mobile and cluster together to attain maximal function (13, 14). Integrin clustering drives the assembly of focal contacts that serve as mechanotransducers and signaling nexuses for cells (5, 15, 16).

Synthetic clustering of multiple copies of the RGD sequence in polyvalent dendritic polymers enhances cell attachment, migration, and targeting (17–20). For optimal effect, clustered ligands should be spaced far enough apart to avoid steric hindrance to binding (integrin receptor diameter, ~10 nm) but close enough to promote synergistic interactions. Integrin ligand spacings on the order of 80 to 140 nm are required for the assembly of focal adhesion domains (21, 22). However, in rats and dogs, coating of implants with individual linear RGD-containing peptides does not promote or enhance implant integration or bone formation compared to the surface treatments that are used in the clinic (23–26), including porous and hydroxyapatite-coated implants. These findings suggest that such RGD-based approaches have limited therapeutic application.

We hypothesized that immobilization of a flexible macromolecular assembly that presents multiple tethered copies of bioligands could promote cellular integrin clustering and signaling and thereby enhance integration of an implant. We therefore tested whether recombinant constructs displaying specified numbers of the 7 to 10 type III repeats of fibronectin ($FNIII_{7–10}$)–binding domain (27) could promote implant integration into bone.

RESULTS

$FNIII_{7–10}$ presents the PHSRN (Pro-His-Ser-Arg-Asn) and RGD integrin-binding sites of fibronectin in an arrangement that results in high binding specificity for integrin $\alpha_5\beta_1$ (23, 28). In previous studies, we have shown that the presentation of $FNIII_{7–10}$ on a substrate enhances osteoprogenitor cell differentiation and implant osseointegration when compared to a coating of simple immobilized RGD-containing oligopeptides (23). By combining the $FNIII_{7–10}$ fragment, a flexible linker derived from tenascin ($TNfnIII_{3–8}$), and a multiplex-forming coiled-coil sequence at the C terminus (Fig. 1A), we assembled the bioadhesive domains into a supramolecular construct that presented defined numbers of copies of the cell-adhesive domain on a flexible linker (Fig. 1A). Constructs presenting one, two, three, or five nanoclustered adhesive ligands were generated with different coiled-coil domains. The linker within the $FNIII_{7–10}$ multimeric construct provided flexibility to allow for the rearrangement of the bioadhesive ligands within a range of about 10 to 50 nm.

We expressed recombinant constructs in *Escherichia coli* and purified them with anion-exchange chromatography. The hydrodynamic radii of the multimers were assessed by dynamic light scattering to verify the assembly of the subunits into the expected dimers, trimers, and pentamers. Size histograms (Fig. 1B) show the expected hydrodynamic radius for the monomer (8.5 nm), dimer (12 nm), trimer (22 nm), and pentamer (41 nm) constructs.

Smaller peaks corresponding to partially assembled multimers were observed for the trimer and pentamer preparations, but these constituted <15% of the total amount of material.

To precisely control the presentation of biological ligands on clinically relevant materials, while preventing nonspecific adsorption of biomacromolecules, we used a nonfouling oligo(ethylene glycol)-substituted polymer brush system on clinical-grade titanium (Ti). This thin polymeric coating, generated by surface-initiated atom transfer radical polymerization of poly[oligo(ethylene glycol) methacrylate] [poly(OEGMA)] brushes on Ti, provides a robust coating that can be engineered to present well-defined densities of covalently tethered biological ligands in a background that is resistant to nonspecific biomacromolecule adsorption and cell adhesion (29). This coating technology is compatible with in vivo applications and can be used to rigorously evaluate biomaterial integration and function in animal models (23). Multimeric $FNIII_{7–10}$ constructs were covalently tethered onto these materials, and the density of tethered multimers was controlled by varying the ligand concentration in solution and measured via surface plasmon resonance (SPR) (fig. S1) (28).

The ability of $\alpha_5\beta_1$ integrin to bind to our multivalent constructs was examined by SPR in a cell-free system. In a first set of experiments, SPR chips coated with polymer brushes were modified with the different multimers to present the same density of the $FNIII_{7–10}$ integrin-binding sites (Fig. 2A) (that is, surfaces modified with five times as much monomer as pentamer present the same density of $FNIII_{7–10}$ ligand). Binding of soluble integrin $\alpha_5\beta_1$ to these surfaces was the same for all multimers. In a complementary set of experiments, polymer-coated SPR chips presenting equimolar densities of constructs were used (Fig. 2B). For the same construct densities, integrin binding increased linearly ($R^2 = 0.994$) with the valency. These results demonstrate that the multivalent constructs support integrin $\alpha_5\beta_1$ binding, that integrin-binding sites within the constructs are accessible for receptor binding, and that they are not subject to steric inhibition.

The effects of ligand clustering on cellular responses were examined by culturing human mesenchymal stem cells under osteogenic conditions (growth medium supplemented with Osteogenic Single-Quots kits) on biomaterials presenting multimeric constructs. These stem cells have the potential to differentiate into various lineages and represent a promising cell source for regenerative medicine (30). Biomaterial surfaces were engineered to present equivalent average density (150 fmol/cm^2) of the $FNIII_{7–10}$ domain as quantified by SPR. Because of differences in molecular weight among constructs, the saturation density of tethered constructs was different for each construct (fig. S1). The density of $FNIII_{7–10}$ used (150 fmol/cm^2) represents the highest density of the integrin-binding domain that could be tethered onto the polymer coating while still having equivalent average densities of the $FNIII_{7–10}$ domain for all of the multimeric constructs. Integrin binding in adherent cells was quantified with a biochemical cross-linking and extraction method (31). Surfaces that presented trimeric and pentameric ligands exhibited twice as much integrin binding as the monomeric and dimeric ligands at equivalent ligand densities ($P < 0.05$) (Fig. 3A). No differences in integrin binding were observed between monomeric and dimeric ligands, or between trimers and pentamers, suggesting a threshold response rather than a monotonic increase with valency. Cells did not adhere to control surfaces that presented no multimeric constructs or in the presence of antibodies against the integrin subunit α_5. Using Ti surfaces coated with passively adsorbed monomeric and pentameric ligands, we also examined the effects of ligand nanoclustering on integrin binding at higher multimer surface densities (fig. S2). Adsorption of multimers on unmodified Ti yielded about five times higher $FNIII_{7–10}$ surface density (680 fmol/cm^2) compared to tethered multimers on polymer brush–coated Ti. Experiments to determine binding of soluble integrin to substrates modified with adsorbed monomer and pentamer constructs confirmed equivalent integrin receptor

accessibility for these coated densities (fig. S2A). Consistent with our observations with ligands tethered onto polymer brushes, cells on surfaces that presented pentameric constructs exhibited greater levels of integrin binding (fig. S2B) and adhesion strength (fig. S3C) than the monomeric ligand at equivalent $FNIII_{7–10}$ densities. Together, these results demonstrate that nanoclustering enhances integrin binding to adhesive ligands presented on biomaterial surfaces.

The differences in binding of soluble integrins (linear with total $FNIII_{7–10}$ density) (Fig. 2B) and cell-bound integrins (enhanced binding to trimer and pentamer over monomer and dimer at equal overall densities of $FNIII_{7–10}$) (Fig. 3A and fig. S2) demonstrate that ligand clustering improves cell-adhesive activity. The effects of ligand clustering on cell signaling were explored further by quantification of phosphorylation of focal adhesion kinase (FAK) by Western blotting (Fig. 3B). FAK is a central signaling molecule that is activated by phosphorylation and is involved in integrin-mediated signal transduction, focal adhesion formation, and the osteogenic differentiation pathway (32). We used a phosphotyrosine-specific antibody to examine the phosphorylation of Y^{397}, a tyrosine autophosphorylation site critical for FAK function. We previously demonstrated that blocking the binding of integrin $\alpha_5\beta_1$ to fibronectin inhibits FAK-Y^{397} phosphorylation and osteoblastic differentiation (23, 33). Here, FAK-Y^{397} exhibited more phosphorylation on pentamer-presenting surfaces than on the other multimer-functionalized materials ($P < 0.05$) (Fig. 3B). This result is consistent with the valency-dependent threshold effects observed for integrin binding.

We next examined the effects of ligand clustering on lineage commitment and osteoblastic differentiation for mesenchymal stem cells. Cells cultured on surfaces displaying trimeric and pentameric bioadhesive ligands exhibited significantly more alkaline phosphatase activity than did cells on materials functionalized with monomeric or dimeric constructs ($P < 0.01$) (Fig. 3C). Deposition of calcium phosphate mineral within a collagen matrix is considered an endpoint marker of differentiation. Mineralization, as measured by Ca^{2+} levels, was up-regulated in human stem cells cultured on biomaterials presenting trimers and pentamers of $FNIII_{7–10}$ compared to substrates functionalized with monomeric and dimeric constructs ($P < 0.04$) (Fig. 3D), in agreement with our results on alkaline phosphatase activity. Together, these results demonstrate that adhesive ligand multivalency (trimers and pentamers) enhanced integrin binding, signaling, and osteoblastic differentiation in human stem cells.

Enhancements of tissue repair and device integration represent the ultimate goal for biomaterial-based therapeutic strategies. As a relevant test of such behavior, we examined the effects of our multivalent ligands on implant osseointegration. Ti rods functionalized with the multimeric constructs ($FNIII_{7–10}$ average density, 150 fmol/cm^2) were press-fit into circular defects drilled into rat proximal tibia (Fig. 4A). This model mimics dental and orthopedic clinical procedures, such as endosteal dental implants and joint arthroplasties, where the mechanical and biological integration of the implant and surrounding bone is critical to function. Therefore, this in vivo model provides a platform to rigorously evaluate the effects of implant coating in a relevant dental and orthopedic setting (23, 34, 35). Tibiae were harvested after 4 and 12 weeks and analyzed for bone-implant contact by histomorphometry (4 weeks) and implant-bone fixation by mechanical testing (4 and 12 weeks). Histological sections revealed more extensive and contiguous bone in close apposition to the trimer- and pentamer-functionalized implants than for the monomer- and dimer-coated implants (Fig. 4B). Control implants presenting poly(OEGMA) brushes without tethered bioadhesive ligands displayed limited bone-implant contact. No evidence of multinucleated cells, fibrous capsule, or chronic inflammation was observed for any of the groups. Histomorphometric analysis demonstrated a 50% increase in bone-implant contact

area for the trimer-and pentamer-functionalized implants compared to monomer-coated rods ($P < 0.04$), a 250% increase compared to the polymer brush–coated Ti in the absence of tethered ligand ($P < 0.01$), and a 75% increase over unmodified Ti (33 ± 3% bone-implant contact), the current clinical standard ($P < 0.02$) (Fig. 4C).

Mechanical fixation provides a rigorous metric of functional implant osseointegration. Pullout mechanical testing at 4 and 12 weeks of implantation revealed ligand valency–dependent differences ($P < 0.01$; Fig. 4D). Trimer- and pentamer-functionalized implants exhibited a 250% enhancement in fixation over monomer- and dimer-tethered implants ($P < 0.002$), and ~400% improvement relative to the unmodified polymer coating ($P < 0.001$). Furthermore, implants presenting trimers and pentamers required twice as much force to be pulled out as did unmodified Ti (17 ± 4.2 N pullout force at 12 weeks, $P < 0.001$), the current clinical standard.

DISCUSSION

Our results demonstrate that clinical implants coated with nanoclustered biological ligands enhance integrin binding and signaling, stem cell differentiation, and in vivo implant integration relative to coatings displaying equivalent densities of monovalent ligand. We attribute the effects of ligand multivalency and clustering on these biological responses to enhancements in binding of integrin $\alpha_5\beta_1$. How does ligand clustering exert its influence over binding to integrins in a cell membrane? For integrins located in the cell membrane, ligand clustering results in greater integrin binding by increasing the local density of ligand and increasing the effective affinity by spatially constraining the receptors to the plane of the membrane. We observed this cooperative binding behavior for integrin receptors in cells but not for freely diffusing soluble receptors. These findings agree with simulations of integrin binding and clustering (36, 37). Our observation of a threshold for optimal binding (trimer and pentamer exhibit greater in vitro and in vivo biological responses than monomer and dimer) is consistent with previous suggestions that a trimer is the minimal matrix complex causing integrin-cytoskeleton connections (27, 38).

Integrin clustering is a critical step in the cell adhesion process that promotes recruitment of cytoskeletal components and activation of signaling molecules (13, 14). Our data show that integrin clustering can be exploited by engineering materials that present well-defined, multivalent adhesive ligands. This affords control over mesenchymal stem cell lineage commitment and differentiation, as well as biomaterial integration. Moreover, our work demonstrates that substrate manipulation alone can be used to directly influence essential functions of the entire tissue, confirming the utility of a material-based strategy in regenerative medicine. The use of recombinant multimeric constructs has important advantages over the stochastic presentation of many other adhesive RGD-based peptides, including the ability to have precise control over valency ligand spacing and integrin-binding specificity. Specifically, this study establishes bioadhesive ligand clustering as a key parameter for the rational engineering of bioactive materials for regenerative medicine and demonstrates methods to exploit this strategy.

MATERIALS AND METHODS

Multimer preparation and characterization

Recombinant multimeric $FNIII_{7–10}$ proteins presenting the central cell-binding domain of fibronectin were expressed as described (27). DNA constructs were transformed into *E. coli* BL21(DE3), and cells were lysed with lysozyme. Protein was precipitated with ammonium sulfate. Pellets were resuspended in buffer (0.02 M tris, 0.1 M NaCl) and run through a Sephacryl 500 column. Peak fractions were then run through a RESOURCE Q column

(Amersham Pharmacia). High-purity proteins were eluted at 0.22 M NaCl (pentamer and trimer), 0.24 M NaCl (dimer), and 0.27 M NaCl (monomer). Dynamic light scattering was performed on purified protein samples dialyzed in ultrapure water at protein concentrations of 2 mg/ml.

Biomaterial supports

Poly(OEGMA) brushes (135 Å thick) were grown on commercial clinical-grade Ti as described (29). For ligand tethering, brushes were first incubated in a 4-nitrophenyl chloroformate (NPC) solution containing triethylamine, followed by incubation in ligand solution for 1 hour, and residual activated NPC sites were quenched in 20 mM glycine in phosphate-buffered saline (PBS). Brush synthesis and functionalization reactions were verified by x-ray photoelectron spectroscopy and Fourier transform infrared spectroscopy. Ligand surface density measurements were obtained via SPR with a Biacore X instrument.

Cells

Human mesenchymal stem cells were obtained from Lonza, cultured in Lonza MSCM and SingleQuots, and passaged every 3 to 4 days before 60% confluency. Osteogenic SingleQuots kits (PT-4120, Lonza) were used in Lonza Basal Medium (replaced every 3 to 4 days) for subsequent osteoblast differentiation assays.

Integrin binding, adhesion, and FAK signaling assays

SPR measurements were conducted with soluble human $\alpha_5\beta_1$ integrin by means of a Biacore X instrument. Gold-coated SIA chips (Biacore) were coated with 50 Å Ti, and brushes were deposited on the surface as described (29). Surfaces were activated with NPC for 20 min. Ligands were tethered on chips by flowing a solution containing them at 8 μl/min for 30 min. A solution (200 μg/ml) of human recombinant soluble $\alpha_5\beta_1$ (R&D Systems) was passed over the multimer-functionalized chips for 10 min in integrin-activating conditions (PBS + 1 mM Mn^{+2}), the surfaces were washed, and the baseline was allowed to stabilize before the amount of bound integrin was quantified. Resonance units (RUs) were converted to surface density values (10 RUs = 1 ng/cm^2).

Integrin binding in cells was quantified with a cross-linking–extraction–reversal procedure with 3,3′-dithiobis[sulfosuccinimidyl propionate] cross-linker (31). For FAK activation assays, human mesenchymal stem cells were plated on multimer-tethered substrates for 2 hours at 37°C under serum-free conditions. Cells were lysed in radioimmunoprecipitation assay buffer [1% Triton X-100, 1% sodium deoxycholate, 0.1% SDS, 150 mM NaCl, 150 mM tris-HCl (pH 7.2), phenylmethylsulfonyl fluoride (350 μg/ml), leupeptin (10 μg/ml), and aprotinin (10 μg/ml)], and equal amounts of total protein were loaded on 8% SDS–polyacrylamide gel electrophoresis (SDS-PAGE) gels, separated by SDS-PAGE, and transferred to nitrocellulose membranes. FAK activation was assessed by subsequent Western blotting with antibodies specific for FAK phosphotyrosines (Invitrogen) and normalized to total FAK levels.

Osseointegration study

Implantations into the tibiae of mature Sprague-Dawley male rats were conducted in accordance with an Institutional Animal Care and Use Committee–approved protocol (35). Ti rods and polymer brushes were prepared as described (23). Multimeric constructs were tethered to yield equimolar densities of the $FNIII_{7–10}$ domain (150 fmol/cm^2). Two 2-mm-diameter defects were drilled into the medial aspect of the proximal tibial metaphysis of each leg, and implants were press-fit into the defects (four implants per animal). After euthanasia, tibiae were explanted and either fixed in neutral buffered formalin (histology) or

wrapped in PBS for immediate mechanical testing. Formalin-fixed tibiae were embedded in poly(methyl methacrylate), dehydrated, and stained with Sanderson's Rapid Bone Stain (Surgipath) and Van Gieson counterstain (Surgipath). This procedure stained mineralized bone (yellow-orange) and soft tissue and osteoid (blue-green). Bone apposition was quantified as the percentage of the implant's surface in contact with the bone, and six to eight fields per implant were quantified. Pullout testing was performed to quantify implant mechanical fixation to surrounding bone tissue with an EnduraTEC Bose ELF 3200. The ends of each excised tibia were secured, and the exposed head of the implant was connected to a load cell via a customized grip apparatus. Preloaded samples (<2 N) were then subjected to a constant pull rate of 0.2 N/s. The pullout force (*N*), parallel to the long axis of implant, was the maximum load achieved before implant detachment or failure.

Statistics

Results are presented as mean ± SEM. Results were analyzed by analysis of variance (ANOVA) in SYSTAT 8.0 (SPSS). If deemed significant, pairwise comparisons were performed with Tukey post hoc test, and a confidence level of 95% was considered significant. In vitro assays were conducted in at least triplicate and replicated in two separate experiments.

Supplementary Material

Refer to Web version on PubMed Central for supplementary material.

Acknowledgments

We thank H. Erickson for providing complementary DNA for fibronectin constructs and M. Mathews for implant machining.

Funding: This work was supported by NIH grants R01 EB-004496 and R01 GM-06591. T.A.P. acknowledges support from the Medtronic Foundation.

REFERENCES AND NOTES

1. Lutolf MP, Hubbell JA. Synthetic biomaterials as instructive extracellular microenvironments for morphogenesis in tissue engineering. Nat Biotechnol. 2005; 23:47–55. [PubMed: 15637621]
2. Langer R, Tirrell DA. Designing materials for biology and medicine. Nature. 2004; 428:487–492. [PubMed: 15057821]
3. Anderson JM, Rodriguez A, Chang DT. Foreign body reaction to biomaterials. Semin Immunol. 2008; 20:86–100. [PubMed: 18162407]
4. Hynes RO. Integrins: Bidirectional, allosteric signaling machines. Cell. 2002; 110:673–687. [PubMed: 12297042]
5. Vogel V, Sheetz MP. Cell fate regulation by coupling mechanical cycles to biochemical signaling pathways. Curr Opin Cell Biol. 2009; 21:38–46. [PubMed: 19217273]
6. Globus RK, Amblard D, Nishimura Y, Iwaniec UT, Kim JB, Almeida EA, Damsky CD, Wronski TJ, van der Meulen MC. Skeletal phenotype of growing transgenic mice that express a function-perturbing form of β1 integrin in osteoblasts. Calcif Tissue Int. 2005; 76:39–49. [PubMed: 15477996]
7. Globus RK, Doty SB, Lull JC, Holmuhamedov E, Humphries MJ, Damsky CH. Fibronectin is a survival factor for differentiated osteoblasts. J Cell Sci. 1998; 111:1385–1393. [PubMed: 9570756]
8. Moursi AM, Globus RK, Damsky CH. Interactions between integrin receptors and fibronectin are required for calvarial osteoblast differentiation in vitro. J Cell Sci. 1997; 110:2187–2196. [PubMed: 9378768]
9. Cheng SL, Lai CF, Blystone SD, Avioli LV. Bone mineralization and osteoblast differentiation are negatively modulated by integrin αvβ3. J Bone Miner Res. 2001; 16:277–288. [PubMed: 11204428]

10. García AJ. Get a grip: Integrins in cell–biomaterial interactions. Biomaterials. 2005; 26:7525–7529. [PubMed: 16002137]
11. García AJ, Reyes CD. Bio-adhesive surfaces to promote osteoblast differentiation and bone formation. J Dent Res. 2005; 84:407–413. [PubMed: 15840774]
12. Ruoslahti E, Pierschbacher MD. New perspectives in cell adhesion: RGD and integrins. Science. 1987; 238:491–497. [PubMed: 2821619]
13. Miyamoto S, Akiyama SK, Yamada KM. Synergistic roles for receptor occupancy and aggregation in integrin transmembrane function. Science. 1995; 267:883–885. [PubMed: 7846531]
14. Miyamoto S, Teramoto H, Coso OA, Gutkind JS, Burbelo PD, Akiyama SK, Yamada KM. Integrin function: Molecular hierarchies of cytoskeletal and signaling molecules. J Cell Biol. 1995; 131:791–805. [PubMed: 7593197]
15. Geiger B, Bershadsky A, Pankov R, Yamada KM. Transmembrane crosstalk between the extracellular matrix and the cytoskeleton. Nat Rev Mol Cell Biol. 2001; 2:793–805. [PubMed: 11715046]
16. Geiger B, Spatz JP, Bershadsky AD. Environmental sensing through focal adhesions. Nat Rev Mol Cell Biol. 2009; 10:21–33. [PubMed: 19197329]
17. Koo LY, Irvine DJ, Mayes AM, Lauffenburger DA, Griffith LG. Co-regulation of cell adhesion by nanoscale RGD organization and mechanical stimulus. J Cell Sci. 2002; 115:1423–1433. [PubMed: 11896190]
18. Maheshwari G, Brown G, Lauffenburger DA, Wells A, Griffith LG. Cell adhesion and motility depend on nanoscale RGD clustering. J Cell Sci. 2000; 113:1677–1686. [PubMed: 10769199]
19. Villard V, Kalyuzhniy O, Riccio O, Potekhin S, Melnik TN, Kajava AV, Rüegg C, Corradin G. Synthetic RGD-containing α-helical coiled coil peptides promote integrin-dependent cell adhesion. J Pept Sci. 2006; 12:206–212. [PubMed: 16103993]
20. Garanger E, Boturyn D, Dumy P. Tumor targeting with RGD peptide ligands—design of new molecular conjugates for imaging and therapy of cancers. Anticancer Agents Med Chem. 2007; 7:552–558. [PubMed: 17896915]
21. Huang J, Grater SV, Corbellini F, Rinck S, Bock E, Kemkemer R, Kessler H, Ding J, Spatz JP. Impact of order and disorder in RGD nanopatterns on cell adhesion. Nano Lett. 2009; 9:1111–1116. [PubMed: 19206508]
22. Massia SP, Hubbell JA. An RGD spacing of 440 nm is sufficient for integrin $\alpha_V\beta_3$-mediated fibroblast spreading and 140 nm for focal contact and stress fiber formation. J Cell Biol. 1991; 114:1089–1100. [PubMed: 1714913]
23. Petrie TA, Raynor JE, Reyes CD, Burns KL, Collard DM, García AJ. The effect of integrin-specific bioactive coatings on tissue healing and implant osseointegration. Biomaterials. 2008; 29:2849–2857. [PubMed: 18406458]
24. Schliephake H, Scharnweber D, Dard M, Rössler S, Sewing A, Meyer J, Hoogestraat D. Effect of RGD peptide coating of titanium implants on periimplant bone formation in the alveolar crest. An experimental pilot study in dogs. Clin Oral Implants Res. 2002; 13:312–319. [PubMed: 12010163]
25. Barber TA, Ho JE, De Ranieri A, Virdi AS, Sumner DR, Healy KE. Peri-implant bone formation and implant integration strength of peptide-modified p(AAM-*co*-EG/AAC) interpenetrating polymer network-coated titanium implants. J Biomed Mater Res A. 2007; 80:306–320. [PubMed: 16960836]
26. Hennessy KM, Clem WC, Phipps MC, Sawyer AA, Shaikh FM, Bellis SL. The effect of RGD peptides on osseointegration of hydroxyapatite biomaterials. Biomaterials. 2008; 29:3075–3083. [PubMed: 18440064]
27. Coussen F, Choquet D, Sheetz MP, Erickson HP. Trimers of the fibronectin cell adhesion domain localize to actin filament bundles and undergo rearward translocation. J Cell Sci. 2002; 115:2581–2590. [PubMed: 12045228]
28. Petrie TA, Capadona JR, Reyes CD, García AJ. Integrin specificity and enhanced cellular activities associated with surfaces presenting a recombinant fibronectin fragment compared to RGD supports. Biomaterials. 2006; 27:5459–5470. [PubMed: 16846640]

29. Raynor JE, Petrie TA, García AJ, Collard DM. Controlling cell adhesion to titanium: Functionalization of poly[oligo(ethylene glycol)methacrylate] brushes with cell-adhesive peptides. Adv Mater. 2007; 19:1724–1728.

30. Pittenger MF, Mackay AM, Beck SC, Jaiswal RK, Douglas R, Mosca JD, Moorman MA, Simonetti DW, Craig S, Marshak DR. Multilineage potential of adult human mesenchymal stem cells. Science. 1999; 284:143–147. [PubMed: 10102814]

31. Keselowsky BG, García AJ. Quantitative methods for analysis of integrin binding and focal adhesion formation on biomaterial surfaces. Biomaterials. 2005; 26:413–418. [PubMed: 15275815]

32. Tamura Y, Takeuchi Y, Suzawa M, Fukumoto S, Kato M, Miyazono K, Fujita T. Focal adhesion kinase activity is required for bone morphogenetic protein—Smad1 signaling and osteoblastic differentiation in murine MC3T3-E1 cells. J Bone Miner Res. 2001; 16:1772–1779. [PubMed: 11585340]

33. Keselowsky BG, Collard DM, García AJ. Integrin binding specificity regulates bio-material surface chemistry effects on cell differentiation. Proc Natl Acad Sci USA. 2005; 102:5953–5957. [PubMed: 15827122]

34. Petrie TA, Reyes CD, Burns KL, García AJ. Simple application of fibronectin–mimetic coating enhances osseointegration of titanium implants. J Cell Mol Med. 2009; 13:2602–2612. [PubMed: 18752639]

35. Reyes CD, Petrie TA, Burns KL, Schwartz Z, García AJ. Biomolecular surface coating to enhance orthopaedic tissue healing and integration. Biomaterials. 2007; 28:3228–3235. [PubMed: 17448533]

36. Irvine DJ, Hue KA, Mayes AM, Griffith LG. Simulations of cell-surface integrin binding to nanoscale-clustered adhesion ligands. Biophys J. 2002; 82:120–132. [PubMed: 11751301]

37. Brinkerhoff CJ, Linderman JJ. Integrin dimerization and ligand organization: Key components in integrin clustering for cell adhesion. Tissue Eng. 2005; 11:865–876. [PubMed: 15998226]

38. Jiang G, Giannone G, Critchley DR, Fukumoto E, Sheetz MP. Two-piconewton slip bond between fibronectin and the cytoskeleton depends on talin. Nature. 2003; 424:334–337. [PubMed: 12867986]

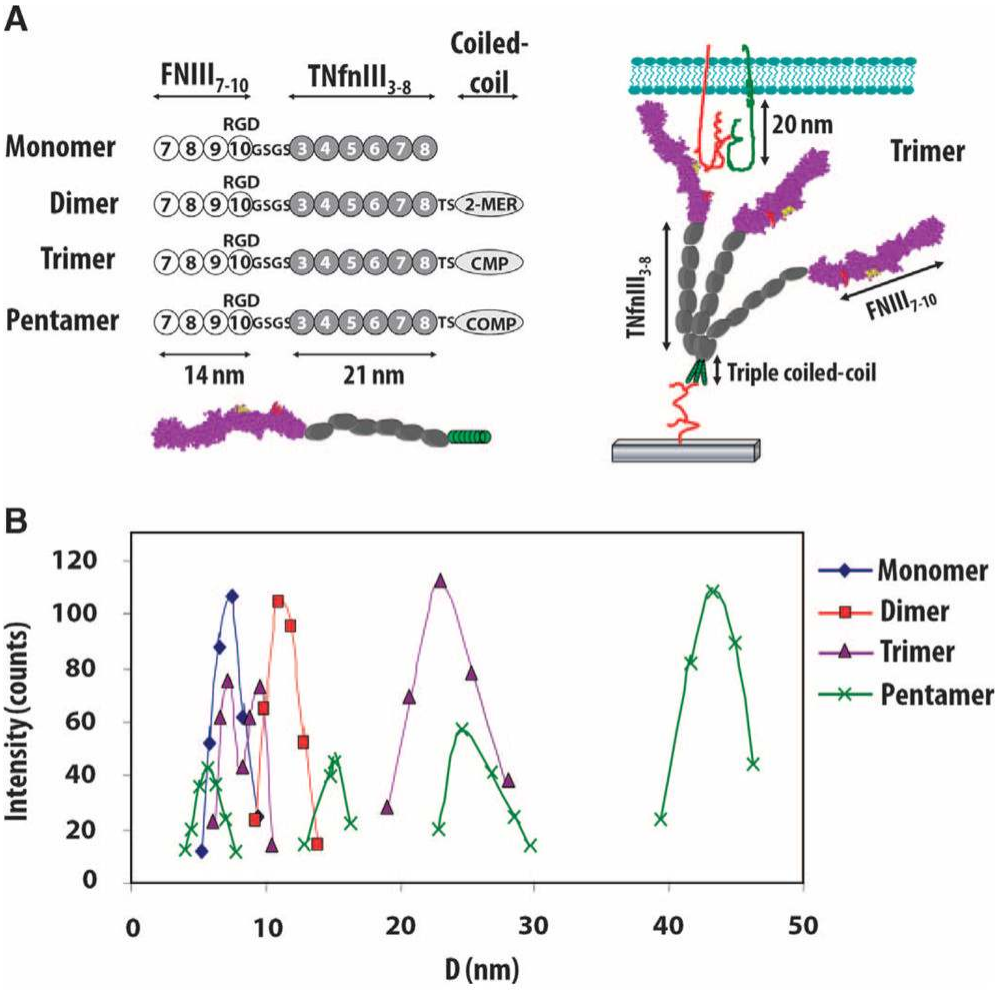

Fig. 1.

Multimeric constructs with precise nanoclustered integrin-binding domains. (**A**) Constructs consisting of the $FNIII_{7–10}$ integrin-binding domain at the N terminus, flexible spacer arm comprising the FNIII domains 3 to 8 from tenascin, and a distinct oligomerization sequence at the C terminus: K6 peptide for dimer, cartilage matrix protein (CMP) for trimer, and cartilage oligomeric matrix protein (COMP) for pentamer. Schematic of trimer tethered to a surface and interacting with integrins via the $FNIII_{7–10}$–binding domain. (**B**) Histograms of construct hydrodynamic diameter (D) for purified multimer fractions. A mixture of complete and incompletely assembled multimers was detected; the majority (>85%) of multimers were completely assembled as the desired dimer, trimer, and pentamer constructs.

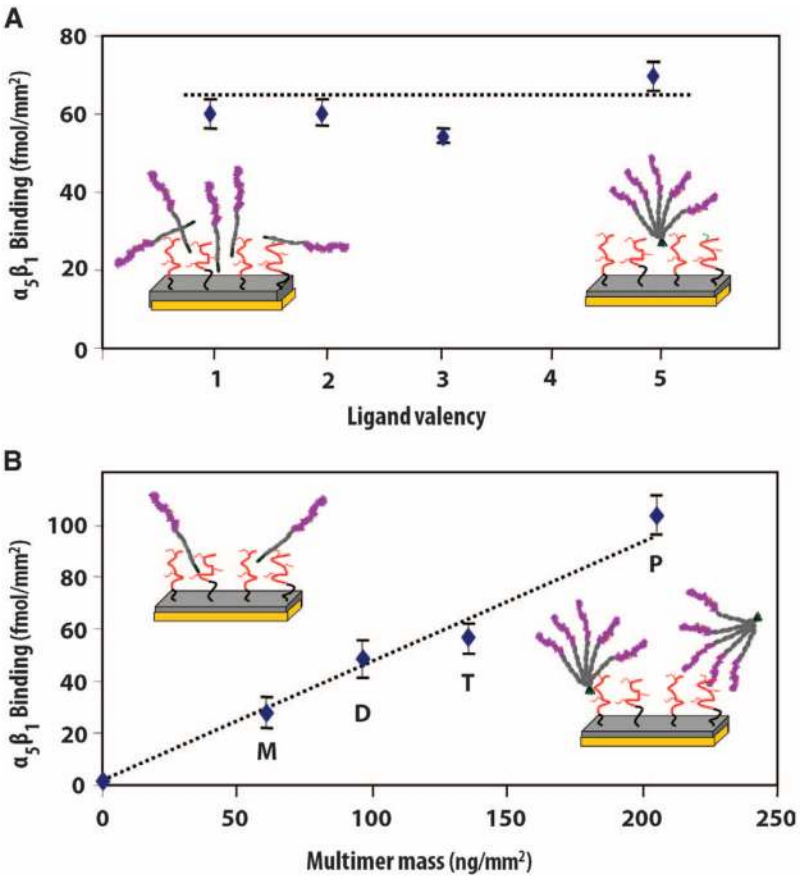

Fig. 2.

The integrin-binding sites within the multivalent ligand constructs are accessible for receptor binding and support robust $\alpha_5\beta_1$ binding. Binding of soluble human $\alpha_5\beta_1$ integrin to multimers immobilized on polymer brushes (orientation uncontrolled). (**A**) Equimolar average densities of $FNIII_{7-10}$–binding domains. (**B**) Surfaces presenting equimolar densities of multimers. Integrin binding increased linearly with ligand valency ($R^2 = 0.994$).

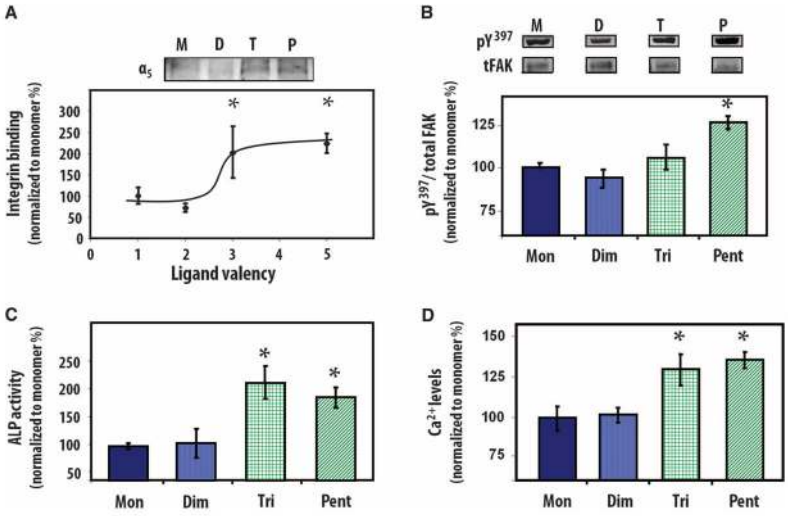

Fig. 3.

Human mesenchymal stem cell responses to biomaterials presenting multivalent adhesive ligands at equimolar average density of $FNIII_{7–10}$ domains. (**A**) Integrin binding to multimeric constructs in whole cells (1 hour, 37°C), showing threshold response [pentamer (P) and trimer (T) versus monomer (M) and dimer (D): $*P < 0.05$, $n = 6$]. (**B**) Phosphorylation of FAK-Y^{397} in whole-cell lysates (2 hours, 37°C) is enhanced on surfaces presenting higher-valency ligands [pentamer (Pent) versus monomer (Mon), dimer (Dim), and trimer (Tri): $*P < 0.05$, $n = 4$]. (**C** and **D**) Biomaterials presenting trimers and pentamers enhance alkaline phosphatase (ALP) activity (pentamer and trimer versus monomer and dimer: $*P < 0.01$) and mineralization as measured by extracellular Ca^{2+} in 14-day cultures of mesenchymal stem cells (pentamer and trimer versus monomer and dimer: $*P < 0.04$).

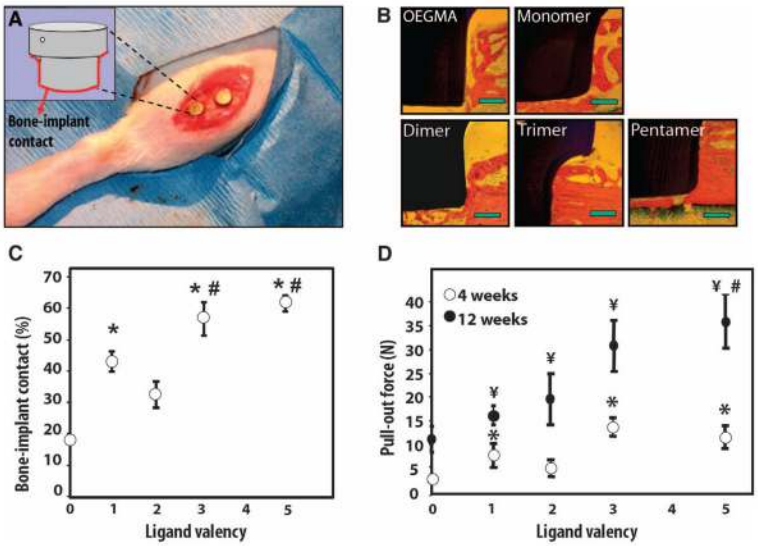

Fig. 4.

Nanoclustered ligand coatings enhance functional in vivo implant osseointegration. (**A**) Bone implantation model for assessment of implant integration by measuring bone-implant contact and mechanical fixation. Photograph shows placement of two implants. (**B**) Micrographs of bone-implant longitudinal sections showing mineralized bone (red/orange) and implant (black) contact. Scale bars, 0.2 mm. (**C**) Quantification of bone-implant contact at 4 weeks after implantation demonstrating valency-dependent enhancements (pentamer versus monomer and dimer: $^{\#}P < 0.04$; pentamer versus no ligand: $^{*}P < 0.0001$, $n = 4$; trimer versus monomer, dimer, and no ligand: $^{*}P < 0.05$, $n = 4$; monomer versus no ligand: $^{*}P < 0.01$, $n = 4$). (**D**) Biomaterials presenting trimers and pentamers significantly increased mechanical fixation (4 weeks: pentamer, trimer, and monomer versus no ligand: $^{*}P < 0.01$, $n = 8$; 12 weeks: pentamer versus monomer and dimer: $^{\#}P < 0.002$, $n = 7$; pentamer, trimer, and monomer versus no ligand: $^{¥}P < 0.01$, $n = 7$).